

2003

Transition Rates via Bethe Ansatz for the Spin-1/2 Planar XXZ Antiferromagnet

Daniel Biegel

Michael Karbach
University of Rhode Island

See next page for additional authors

Follow this and additional works at: https://digitalcommons.uri.edu/phys_facpubs

Terms of Use

All rights reserved under copyright.

Citation/Publisher Attribution

Biegel, D., Karbach, M., & Müller, G. (2003). Transition rates via Bethe ansatz for the spin-1/2 planar XXZ antiferromagnet. *Journal of Physics A*, 36, 5361-5368.

Available at: <http://dx.doi.org/10.1088/0305-4470/36/20/301>

This Article is brought to you for free and open access by the Physics at DigitalCommons@URI. It has been accepted for inclusion in Physics Faculty Publications by an authorized administrator of DigitalCommons@URI. For more information, please contact digitalcommons@etal.uri.edu.

Authors

Daniel Biegel, Michael Karbach, and Gerhard Müller

Transition rates via Bethe ansatz for the spin-1/2 planar XXZ antiferromagnet

Daniel Biegel*, Michael Karbach*[†], and Gerhard Müller[†]

*Bergische Universität Wuppertal, Fachbereich Physik, D-42097 Wuppertal, Germany

[†]Department of Physics, University of Rhode Island, Kingston RI 02881-0817, USA

PACS numbers: 75.10.-b

Abstract. A novel determinantal representation for matrix elements of local spin operators between Bethe wave functions of the one-dimensional $s = \frac{1}{2}$ XXZ model is used to calculate transition rates for dynamic spin structure factors in the planar regime. In a first application, high-precision numerical data are presented for lineshapes and band edge singularities of the in-plane (xx) two-spinon dynamic spin structure factor.

1. Introduction

The importance of the spinon quasiparticle for the understanding of the quantum fluctuations in integrable quantum spin chains is established on rigorous grounds and further supported by experiments probing the dynamical properties of quasi-one-dimensional magnetic compounds at low temperatures. Consider the familiar and widely studied $s = \frac{1}{2}$ XXZ antiferromagnet,

$$H \doteq J \sum_{n=1}^N (S_n^x S_{n+1}^x + S_n^y S_{n+1}^y + \Delta S_n^z S_{n+1}^z), \quad (1.1)$$

with $J > 0, \Delta > 0$. Its ground state for even N can be configured as the physical vacuum for spinons and its entire spectrum can be generated via systematic creation of spinon pairs, for example, in the framework of the algebraic Bethe ansatz [1].

Theoretical and experimental evidence points to the dominance of two-spinon excitations in the low-temperature spin dynamics of the XXZ antiferromagnet [2, 3, 4, 5, 6]. The exact two-spinon dynamic structure factor for the spin fluctuations perpendicular to the antiferromagnetic long-range order in the axial regime $\Delta > 1$ was recently calculated via algebraic analysis [7, 8]. This method of exact analysis is not readily applicable in the planar regime $\Delta < 1$, but exact results for the case of isotropic exchange ($\Delta = 1$) can be inferred as a limiting case. Extending the exact analysis of dynamic structure factors into the planar regime has been a tantalizing challenge ever since.

Remarkable advances in the determination of matrix elements from Bethe wave functions opened up new and promising avenues for the calculation of dynamical properties of the XXZ model. Of critical importance has been the recent work

of Kitanine, Maillet, and Terras [9] and the earlier work of Korepin and Izergin [10, 11, 12], which accomplished a reduction of the norms of Bethe wave functions and of matrix elements (form factors) for the local spin operators S_n^α , $\alpha = x, y, z$, to determinants. We have already used their formulas to calculate explicit expressions for transition rates of spin fluctuation operators between eigenstates of the XXX model ($\Delta = 1$) and have applied them to calculate lineshapes of dynamic spin structure factors in a magnetic field [13]. Here we present corresponding exact expressions for the XXZ model in the planar regime ($0 < \Delta < 1$) with an application to the in-plane two-spinon dynamic spin structure factor. Related projects, which focus on out-of-plane spin fluctuations, dimer fluctuations, XX limit ($\Delta = 0$), four-spinon structure factors, axial regime, and $T > 0$ dynamics are in progress [14].

2. Bethe ansatz equations

The Bethe wave function of every eigenstate in the invariant subspace with z -component $S_T^z = N/2 - r$ of the total spin is specified by a set of rapidities z_1, \dots, z_r , which are solutions of the Bethe ansatz equations [15, 16]

$$N \arctan \left(\cot \frac{\gamma}{2} \tanh \frac{z_i}{2} \right) = \pi I_i + \sum_{j \neq i}^r \arctan \left(\cot \gamma \tanh \frac{z_i - z_j}{2} \right), \quad i = 1, \dots, r \quad (2.1)$$

with anisotropy parameter

$$\gamma \doteq \arccos \Delta \quad (0 < \gamma < \pi). \quad (2.2)$$

Different solutions within this subspace are distinguished by different sets of Bethe quantum numbers $\{I_i\}$. It is useful to further distinguish solutions with only real magnon momenta k_i and solutions where some or all k_i are complex. The relation between the magnon momenta k_i and the rapidities z_i is

$$\tanh \frac{z_i}{2} = y_i \doteq \tan \frac{\gamma}{2} \cot \frac{k_i}{2}. \quad (2.3)$$

The transition rate expressions to be presented below are constructed to hold for all Bethe ansatz solutions with real k_i . The generalizations necessary to cover also solutions with complex k_i are straightforward [17].

It turns out that even in the restricted set of solutions with real k_i some of the rapidities may not be real, namely those with $|\tanh(z_i/2)| > 1$, which poses a problem in root-finding algorithms. To circumnavigate the problem we introduce alternate rapidities y_i defined in (2.3). They stay real for all eigenstates with real k_i . The Bethe ansatz equations for the y_i read

$$N \arctan \left(y_i \cot \frac{\gamma}{2} \right) = \pi I_i + \sum_{j \neq i}^r \arctan \left(\cot \gamma \frac{y_i - y_j}{1 - y_i y_j} \right), \quad i = 1, \dots, r. \quad (2.4)$$

The wave number and energy of any given solution are

$$k = \pi r - \frac{2\pi}{N} \sum_{i=1}^r I_i, \quad (2.5)$$

$$\frac{E - E_F}{J} = - \sum_{i=1}^r (\Delta - \cos k_i) = - \sum_{i=1}^r \frac{\sin^2 \gamma}{\cosh z_i - \cos \gamma}, \quad (2.6)$$

where $E_F \equiv N\Delta/4$ is the energy of the reference state $|\uparrow\uparrow \cdots \uparrow\rangle$.

3. Matrix elements

In generalization to the results presented in Ref. [13] for $\Delta = 1$ we use the formulas for matrix elements $\langle \psi_0 | S_n^\mu | \psi_\lambda \rangle$ from Kitanine, Maillet, and Terras [9] and the norms $\|\psi_\lambda\|$ from Korepin [10] of Bethe wave functions with real k_i to calculate transition rates

$$M_\lambda^\mu(q, \gamma) \doteq \frac{|\langle \psi_0 | S_q^\mu | \psi_\lambda \rangle|^2}{\|\psi_0\|^2 \|\psi_\lambda\|^2}, \quad \mu = z, +, - \quad (3.1)$$

from the ground state of H for the operators

$$S_q^\mu = \frac{1}{\sqrt{N}} \sum_n e^{iqn} S_n^\mu, \quad \mu = z, +, -. \quad (3.2)$$

They probe the parallel ($\mu = z$) and the perpendicular ($\mu = +, -$) spin fluctuations at zero temperature. An important and largely unanticipated feature is that the determinantal expressions become much simpler in reciprocal space. For the parallel spin fluctuations our calculations yield the following results:

$$M_\lambda^z(q) = \frac{N}{4} \frac{\mathcal{L}_r(\{z_i\})}{\mathcal{L}_r(\{z_i^0\})} \mathcal{K}_r(\{z_i^0\}) \mathcal{K}_r(\{z_i\}) \frac{|\det(\mathbf{H} - \mathbf{P})|^2}{\det \mathbf{K}(\{z_i\}) \det \mathbf{K}(\{z_i^0\})}, \quad (3.3)$$

where

$$\mathcal{L}_r(\{z_i\}) \doteq \prod_{i=1}^r \kappa(z_i), \quad \mathcal{K}_r(\{z_i\}) \doteq \prod_{i < j}^r |K(z_i - z_j)|, \quad (3.4)$$

$$\mathbf{H}_{ab} \doteq \frac{i}{2} \frac{\sin \gamma}{\sinh[(z_a^0 - z_b)/2]} \left(\prod_{j \neq a}^r G(z_j^0 - z_b) - d(z_b) \prod_{j \neq a}^r G^*(z_j^0 - z_b) \right), \quad (3.5)$$

$$\mathbf{P}_{ab} \doteq i2\kappa(z_a^0) \prod_{j=1}^r G(z_j - z_b), \quad a, b = 1, \dots, r, \quad (3.6)$$

$$G(z) \doteq \sinh(z/2) \cot \gamma + i \cosh(z/2), \quad (3.7)$$

$$d(z) \doteq \left(\frac{\tanh(z/2) \cot(\gamma/2) - i}{\tanh(z/2) \cot(\gamma/2) + i} \right)^N, \quad (3.8)$$

$$\mathbf{K}_{ab} \doteq \begin{cases} K(z_a - z_b) \cos \gamma & : a \neq b \\ N\kappa(z_a) - \cos \gamma \sum_{j \neq a}^r K(z_a - z_j) & : a = b \end{cases}, \quad (3.9)$$

$$\kappa(z) \doteq \frac{1}{2} \frac{\sin^2 \gamma}{\sinh^2(z/2) + \sin^2(\gamma/2)}, \quad (3.10)$$

$$K(z) \doteq \frac{\sin^2 \gamma}{\sinh^2(z/2) + \sin^2 \gamma}. \quad (3.11)$$

The corresponding results for the perpendicular spin fluctuations are

$$M_\lambda^\pm(q) = \left(\frac{\mathcal{L}_r(\{z_i^0\})}{\mathcal{L}_{r\pm 1}(\{z_i\})} \right)^{\pm 1} \mathcal{K}_r(\{z_i^0\}) \mathcal{K}_{r\pm 1}(\{z_i\}) \frac{N |\det \mathbf{H}^\pm|^2}{\det \mathbf{K}(\{z_i\}) \det \mathbf{K}(\{z_i^0\})}, \quad (3.12)$$

where

$$\begin{aligned} \mathbf{H}_{ab}^+ &\doteq \frac{i}{2} \frac{\sin \gamma}{\sinh[(z_a - z_b^0)/2]} \left(\prod_{j \neq a}^{r+1} G(z_j - z_b^0) - d(z_b^0) \prod_{j \neq a}^{r+1} G^*(z_j - z_b^0) \right), \\ \mathbf{H}_{a,r+1}^+ &\doteq i\kappa(z_a), \quad a = 1, \dots, r+1, \quad b = 1, \dots, r, \\ \mathbf{H}_{ab}^- &\doteq \frac{i}{2} \frac{\sin \gamma}{\sinh[(z_a^0 - z_b)/2]} \left(\prod_{j \neq a}^r G(z_j^0 - z_b) - d(z_b) \prod_{j \neq a}^r G^*(z_j^0 - z_b) \right), \\ \mathbf{H}_{ar}^- &\doteq i\kappa(z_a^0), \quad a = 1, \dots, r, \quad b = 1, \dots, r-1. \end{aligned} \quad (3.13)$$

In the combined limits $\gamma \rightarrow 0$, $z_i \rightarrow 0$, $z_i/\gamma \rightarrow z'_i$, we recover term by term the results reported in Ref. [13] for the XXX model ($\Delta = 1$). In the XX limit ($\Delta = 0$) considerable simplifications occur in the transition rate expressions but extreme care must be exercised in their applications because of singularities in the Bethe ansatz equations. These singularities manifest themselves, for example, in the occurrence of *critical* pairs of rapidities y_i, y_j in Eqs. (2.4) with the property $\lim_{\gamma \rightarrow 0} y_i y_j = 1$ [18, 19, 20]. Results for the XX model are forthcoming [14].

More compact expressions for the results (3.3) and (3.12) can be obtained as follows. Replacing (3.9) by the matrix

$$\bar{\mathbf{K}}_{ab} \doteq \begin{cases} \frac{\cos \gamma}{N} \frac{K(z_a - z_b)}{\kappa(z_a)} & : a \neq b \\ 1 - \frac{\cos \gamma}{N} \sum_{j \neq a}^r \frac{K(z_a - z_j)}{\kappa(z_a)} & : a = b \end{cases} \quad (3.15)$$

allows us to extract a factor N^r from $\det \mathbf{K}$:

$$\det \mathbf{K}(\{z_i\}) = N^r \mathcal{L}_r(\{z_i\}) \det \bar{\mathbf{K}}(\{z_i\}). \quad (3.16)$$

Using the Bethe ansatz equations in the algebraic form

$$d(z_i) = - \prod_{j=1}^r \frac{G^*(z_i - z_j)}{G(z_i - z_j)} \quad (3.17)$$

again in \mathbf{H}_{ab} , \mathbf{P}_{ab} , and \mathbf{H}_{ab}^\pm , further simplifies these matrices. The consolidated expressions then read

$$M_\lambda^z(q) = \frac{N \mathcal{K}_r(\{z_i^0\})}{4 \mathcal{K}_r(\{z_i\})} \frac{|\det(\Gamma - \frac{2}{N} \mathbf{1})|^2}{\det \mathbf{K}(\{z_i^0\}) \det \mathbf{K}(\{z_i\})}, \quad (3.18)$$

$$M_\lambda^\pm(q) = \left(\frac{\mathcal{K}_{r\pm 1}(\{z_i\})}{\mathcal{K}_r(\{z_i^0\})} \right)^{\pm 1} \frac{|\det \Gamma^\pm|^2}{\det \bar{\mathbf{K}}(\{z_i\}) \det \bar{\mathbf{K}}(\{z_i^0\})}, \quad (3.19)$$

where

$$\begin{aligned} \Gamma_{ab} &\doteq F_N(z_a^0, z_b) \left(\frac{1}{G(z_a^0 - z_b)} \prod_{j=1}^r \frac{G(z_j^0 - z_b)}{G(z_j - z_b)} + \frac{1}{G^*(z_a^0 - z_b)} \prod_{j=1}^r \frac{G^*(z_j^0 - z_b)}{G^*(z_j - z_b)} \right), \\ \Gamma_{ab}^+ &\doteq F_N(z_a, z_b^0) \left(\frac{G(z_{r+1} - z_b^0)}{G(z_a - z_b^0)} \prod_{j=1}^r \frac{G(z_j - z_b^0)}{G(z_j^0 - z_b^0)} + \frac{G^*(z_{r+1} - z_b^0)}{G^*(z_a - z_b^0)} \prod_{j=1}^r \frac{G^*(z_j - z_b^0)}{G^*(z_j^0 - z_b^0)} \right), \\ \Gamma_{a,r+1}^+ &\doteq 1, \quad a = 1, \dots, r+1, \quad b = 1, \dots, r, \end{aligned} \quad (3.20)$$

$$(3.21)$$

$$\Gamma_{ab}^- \doteq F_N(z_a^0, z_b) \left(\frac{G(z_r^0 - z_b)}{G(z_a^0 - z_b)} \prod_{j=1}^{r-1} \frac{G(z_j^0 - z_b)}{G(z_j - z_b)} + \frac{G^*(z_r^0 - z_b)}{G^*(z_a^0 - z_b)} \prod_{j=1}^{r-1} \frac{G^*(z_j^0 - z_b)}{G^*(z_j - z_b)} \right),$$

$$\Gamma_{ar}^- \doteq 1, \quad a = 1, \dots, r, \quad b = 1, \dots, r-1, \quad (3.22)$$

$$F_N(z, z') \doteq \frac{\sin^2(\gamma/2) + \sinh^2(z/2)}{N \sin \gamma \sinh((z - z')/2)}, \quad (3.23)$$

$$\mathbf{1} \equiv \begin{pmatrix} 1 & \cdots & 1 \\ \vdots & \ddots & \vdots \\ 1 & \cdots & 1 \end{pmatrix}.$$

In the isotropic limit $\gamma \rightarrow 0$ we can use the results (3.18)-(3.20) with

$$F_N(z, z') \doteq \frac{1 + z^2}{2N(z - z')}, \quad (3.24)$$

and the other ingredients as defined in [13].

The corresponding results for $M_{\lambda}^z(q)$ and $M_{\lambda}^{\pm}(q)$ expressed in terms of the rapidities y_i are equally compact [14]. For applications involving excitations with real magnon momenta k_i , we solve the Bethe ansatz equations (2.4) and calculate transition rates from (3.18) and (3.19).

4. Two-spinon dynamic structure factor

To demonstrate the practicality and usefulness of the newly derived transition rate expressions, we present high-precision data for the two-spinon part of the $T = 0$ dynamic structure factor

$$S_{-+}(q, \omega) = 2\pi \sum_{\lambda} M_{\lambda}^{-}(q) \delta(\omega - \omega_{\lambda}), \quad (4.1)$$

which captures the in-plane spin fluctuations. The state $|\psi_0\rangle$ in (3.1) is the XXZ ground state (spinon vacuum). It has quantum number $S_T^z = 0$ and is characterized by the solutions of Eqs. (2.4) for the set of $r = N/2$ Bethe quantum numbers $I_i^{(0)} = -(N+2)/4 + i, i = 1, \dots, N/2$. Excited states containing two spinons with parallel spins are known to account for a major contribution to the in-plane spin fluctuations [3].

The number of two-spinon states with $S_T^z = 1$ is $\frac{1}{8}N(N+2)$. Their $r = N/2 - 1$ Bethe quantum numbers, which are integers for odd r and half-integers for even r , comprise all configurations

$$-\frac{N}{4} \leq I_1 < I_2 < \cdots < I_r \leq \frac{N}{4}. \quad (4.2)$$

These states are described by real solutions of Eqs. (2.4). For $N \rightarrow \infty$ they form a continuum in (q, ω) -space with boundaries [15, 3]

$$\epsilon_L(q) = \frac{\pi J \sin \gamma}{2\gamma} |\sin q|, \quad \epsilon_U(q) = \frac{\pi J \sin \gamma}{\gamma} \left| \sin \frac{q}{2} \right|. \quad (4.3)$$

The scaled density of two-spinon states constructed from $D^{(2)}(q, \omega_{\lambda}) \equiv 2\pi/[N(\omega_{\lambda+1} - \omega_{\lambda})]$ for the energy-sorted sequence of two-spinon excitations at fixed q and finite N turns into the function

$$D^{(2)}(q, \omega) = [\epsilon_U^2(q) - \omega^2]^{-1/2} \quad (4.4)$$

for $\epsilon_L(q) \leq \omega \leq \epsilon_U(q)$ in the limit $N \rightarrow \infty$. For the two-spinon part of the dynamic spin structure factor we use the product representation

$$S_{-+}^{(2)}(q, \omega) = M_{-+}^{(2)}(q, \omega) D^{(2)}(q, \omega) \quad (4.5)$$

as discussed in a previous application of a similar nature [21]. The first factor represents the scaled transition rates $M_{-+}^{(2)}(q, \omega) = N |\langle G | S_q^- | \lambda \rangle|^2$ between the ground state and the two-spinon states (4.2).

Here we focus on the lineshape and on the singularity structure of $S_{-+}^{(2)}(q, \omega)$ at $q = \pi$, where the spectral threshold is at $\omega = 0$. In Fig. 1 we show $N = 512$ data for the transition rate function $M_{-+}^{(2)}(\pi, \omega)$ at $\Delta = 0.1, 0.3, \dots, 0.9$. The data indicate an infrared divergence and exhibit a monotonically decreasing ω -dependence toward zero intensity at the upper band edge. The inset to Fig. 1 zooms into the behavior near $\epsilon_U(\pi)$. The data points approach zero linearly with a slope that becomes smaller with decreasing Δ . A linear behavior was already established via algebraic analysis for the case $\Delta = 1$ [7].

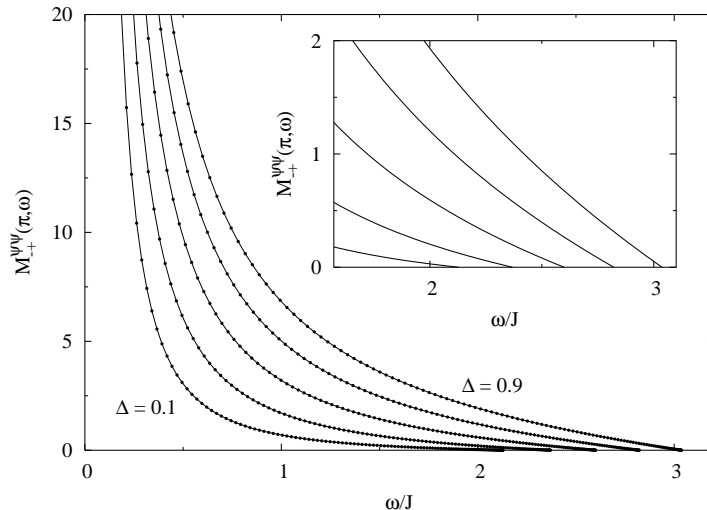


Figure 1. Scaled transition rates between the XXZ ground state and the two-spinon states at $q = \pi$ for $N = 512$ and $\Delta = 0.1, 0.3, \dots, 0.9$. The inset shows the same data again for ω near $\epsilon_U(\pi)$ on a different scale.

The spectral-weight distribution of the two-spinon contribution to $S_{-+}(\pi, \omega)$ is then inferred via product representation (4.5) from the transition rate data and the two-spinon density of states (4.4). The results are shown in Fig. 2. The divergent density of states (4.4) at $\omega = \epsilon_U(\pi)$ converts the linear cusp of the function $M_{-+}^{(2)}(\pi, \omega)$ into a square-root cusp in the function $S_{-+}^{(2)}(\pi, \omega)$ as is best visible in the inset. The Δ -dependent exponent of the power-law singularity is exactly known [22, 23]:

$$S_{-+}(\pi, \omega) \sim \omega^{-1-\gamma/\pi}. \quad (4.6)$$

This non-universal critical singularity is accurately reflected by the $N = 512$ data as is demonstrated by a data fit at low frequencies for each lineshape.

In summary, the availability of determinantal transition rate formulas opens up a whole new area of applications of the Bethe ansatz with enormous potential for

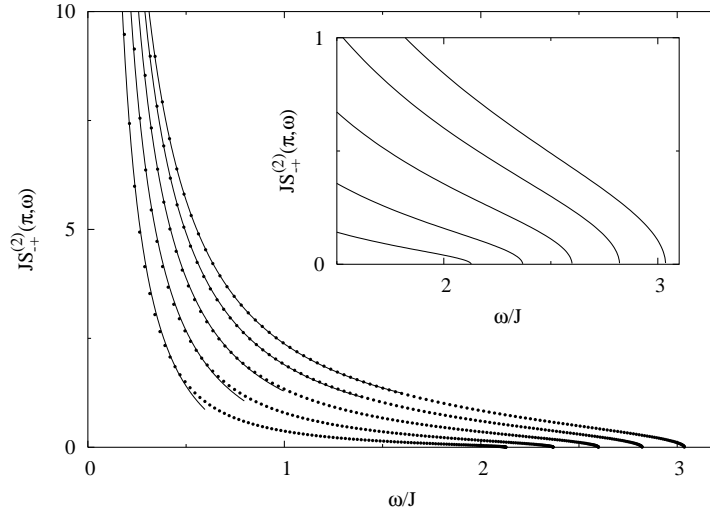


Figure 2. Lineshape at $q = \pi$ of the two-spinon contribution to $S_{-+}(q, \omega)$. The dots represent data for $N = 512$ at $\Delta = 0.1, 0.3, \dots, 0.9$ (left to right). The lines are two-parameter fits $a\omega^{-1-\gamma/\pi} + b$ (over the interval shown) with the exactly known exponent from Eq. (4.6) for $N = \infty$. The inset shows the $N = 512$ data again for ω near $\epsilon_U(\pi)$ on a different scale.

important new results, among them results of relevance for experiments (neutron scattering, NMR) on quasi-one-dimensional magnetic insulators.

Acknowledgments

Financial support from the DFG Schwerpunkt *Kollektive Quantenzustände in elektronischen 1D Übergangsmetallverbindungen* (for M.K.) is gratefully acknowledged. M.K. thanks Prof. Dr. Frommer and Prof. Dr. Fabricius for useful discussions. D.B. thanks Dr. Fledderjohann for useful discussions.

References

- [1] Faddeev L D and Takhtajan L A, 1984 *J. Soviet. Math.* **24** 241
- [2] Ishimura N and Shiba H, 1980 *Prog. Theor. Phys.* **63** 743
- [3] Müller G, Thomas H, Puga M W and Beck H, 1981 *J. Phys. C: Solid St. Phys.* **14** 3399
- [4] Goff J P, Tennant D A and Nagler S E, 1995 *Phys. Rev. B* **52** 15992
- [5] Hammar P R, Stone M B, Reich D H, Broholm C et al., 1999 *Phys. Rev. B* **59** 1008
- [6] Tennant D A, Cowley R A, Nagler S E and Tselik A M, 1995 *Phys. Rev. B* **52** 13368
- [7] Karbach M, Müller G, Bougourzi A H, Fledderjohann A et al., 1997 *Phys. Rev. B* **55** 12510
- [8] Bougourzi A H, Karbach M and Müller G, 1998 *Phys. Rev. B* **57** 11429
- [9] Kitanine N, Maillet J M and Terras V, 1999 *Nucl. Phys. B* **554** 647
- [10] Korepin V E, 1982 *Commun. Math. Phys.* **86** 391
- [11] Izergin A G and Korepin V E, 1985 *Commun. Math. Phys.* **99** 271
- [12] Korepin V E, Bogoliubov N M and Izergin A G, *Quantum Inverse Scattering Method and Correlation Functions* (Cambridge University Press, Cambridge, 1993)
- [13] Biegel D, Karbach M and Müller G, 2002 *Europhys. Lett.* **59** 882
- [14] D. Biegel, M. Karbach, G. Müller, and K. Wiele (unpublished).
- [15] des Cloizeaux J and Gaudin M, 1966 *J. Math. Phys.* **7** 1384
- [16] The rapidities used in Ref. [9] are $\lambda_j = (z_j - i\gamma)/2$

- [17] The most challenging part handling complex solutions is finding the complex roots of the Bethe ansatz equations.
- [18] Biegel D, 2000 *Das eindimensionale Spin-1/2 XX-Modell als Grenzfall des XXZ-Modells*. Diplomarbeit, Bergische Universität Gesamthochschule Wuppertal
- [19] Deguchi T, Fabricius K and McCoy B M, 2001 *J. Stat. Phys.* **102** 701
- [20] Fabricius K and McCoy B M, 2001 *J. Stat. Phys.* **103** 647 ; **104** 573
- [21] Karbach M and Müller G, 2000 *Phys. Rev. B* **62** 14871
- [22] Luther A and Peschel I, 1975 *Phys. Rev. B* **12** 3908
- [23] Fledderjohann A, Gerhardt C, Mütter K H, Schmitt A et al., 1996 *Phys. Rev. B* **54** 7168